Polygenic Risk Scores Validated in Patient-Derived Cells Stratify for Mitochondrial Subtypes of Parkinson's Disease

Giuseppe Arena, PhD [iD],[1†] Zied Landoulsi, PhD,[1†] Dajana Grossmann, PhD,[1,2] Thomas Payne, PhD,[3] Armelle Vitali, MSc,[1] Sylvie Delcambre, PhD,[1] Alexandre Baron, MSc,[1] Paul Antony, PhD [iD],[1] Ibrahim Boussaad, PhD,[1] Dheeraj Reddy Bobbili, PhD [iD],[1] Ashwin Ashok Kumar Sreelatha, MSc, MTech,[4] Lukas Pavelka, MD,[1,5,6] Nico J Diederich, MD,[7] Christine Klein, MD [iD],[8] Philip Seibler, PhD,[8] Enrico Glaab, PhD,[1] Thomas Foltynie, PhD,[9] Oliver Bandmann, PhD [iD],[3] Manu Sharma, PhD [iD],[4] Rejko Krüger, MD [iD],[1,5,6‡] Patrick May, PhD [iD],[1‡] and Anne Grünewald, PhD, [iD][1,8‡] on behalf of the NCER-PD and COURAGE-PD Consortia

Objective: The aim of our study is to better understand the genetic architecture and pathological mechanisms underlying neurodegeneration in idiopathic Parkinson's disease (iPD). We hypothesized that a fraction of iPD patients may harbor a combination of common variants in nuclear-encoded mitochondrial genes ultimately resulting in neurodegeneration.

Methods: We used mitochondria-specific polygenic risk scores (mitoPRSs) and created pathway-specific mitoPRSs using genotype data from different iPD case–control datasets worldwide, including the Luxembourg Parkinson's Study (412 iPD patients and 576 healthy controls) and COURAGE-PD cohorts (7,270 iPD cases and 6,819 healthy controls). Cellular models from individuals stratified according to the most significant mitoPRS were subsequently used to characterize different aspects of mitochondrial function.

Results: Common variants in genes regulating *Oxidative Phosphorylation (OXPHOS-PRS)* were significantly associated with a higher PD risk in independent cohorts (Luxembourg Parkinson's Study odds ratio, OR = 1.31[1.14–1.50],

p-value = 5.4e-04; COURAGE-PD OR = 1.23[1.18–1.27], *p*-value = 1.5e-29). Functional analyses in fibroblasts and induced pluripotent stem cells-derived neuronal progenitors revealed significant differences in mitochondrial respiration between iPD patients with high or low *OXPHOS*-PRS (*p*-values < 0.05). Clinically, iPD patients with high *OXPHOS*-PRS have a significantly earlier age at disease onset compared to low-risk patients (false discovery rate [FDR]-adj *p*-value = 0.015), similar to prototypic monogenic forms of PD. Finally, iPD patients with high *OXPHOS*-PRS responded more effectively to treatment with mitochondrially active ursodeoxycholic acid.

Interpretation: *OXPHOS*-PRS may provide a precision medicine tool to stratify iPD patients into a pathogenic subgroup genetically defined by specific mitochondrial impairment, making these individuals eligible for future intelligent clinical trial designs.

Parkinson's disease (PD) is the fastest growing and as yet incurable neurodegenerative disease, affecting about 1–2% of the population over the age of 60.[1] PD patients typically display bradykinesia with rigidity and/or resting tremor accompanied by a heterogeneous panel of non-motor symptoms (e.g., sleep disturbance, mood disorders, cognitive changes, and autonomic dysfunction). Motor symptoms are mostly caused by disrupted dopamine signaling in the striatum due to loss of dopaminergic neurons (DANs) in the *substantia nigra pars compacta* of the brain. Typical proteinaceous inclusions (i.e., Lewy bodies), composed of α-synuclein, ubiquitin, and other aggregated proteins or organelles, are observed in the surviving DANs.[2] The etiology of PD is complex and influenced by both environmental and genetic factors. Monogenic familial forms, ascribable to single mutations in autosomal dominant (e.g., *SNCA*, *LRRK2*, *VPS35*) or recessive (*PRKN*, *PINK1*, *PARK7*) genes, account for approximately 5–10% of all PD cases.[3] However, the contribution of genetics in the remaining 90–95% of patients with idiopathic PD (iPD) remains poorly understood, and disease susceptibility may be influenced by the synergistic effect of multiple common low-risk genetic variants.[4] To unravel this "missing heritability", systematic approaches based on polygenic risk scores (PRSs) have been proposed in recent years, aimed at identifying individuals with a higher risk to develop PD.[5] PRSs are calculated as the sum of common risk single nucleotide variants (SNVs) weighted by their genome-wide associated studies (GWAS) effect sizes.[6] Applying PRS to a limited number of genes that regulate biological functions known to be altered in PD could potentially reveal a relationship between the pathways involved and their impact in determining the clinical phenotype. Such an approach would allow the stratification of patients according to the underlying pathological mechanisms, thus enabling precision medicine therapeutic approaches.[5]

There is convincing and longstanding evidence that points to mitochondrial dysfunction as an early and causative event in PD pathogenesis. Indeed, both epidemiological studies on humans exposed to pesticides as well as toxin-induced PD models support a primary role for impaired mitochondrial electron transport chain (ETC) activity, as suggested by the selective degeneration of DANs following mitochondrial complex I disruption.[7,8] Moreover, molecular genetic studies in PD families revealed that proteins mutated in early-onset forms (i.e., PINK1 and Parkin) regulate mitochondrial function or even localize to mitochondria.[9] Hallmarks of mitochondrial dysfunction have also been observed in cellular models established from iPD patients, showing defective oxidative phosphorylation (OXPHOS), increased oxidative stress, and mitochondrial DNA (mtDNA) damage.[10–12] Neurodegeneration in such iPD patients cannot be explained by ageing or environmental factors alone,[13] which possibly implies the existence of pathogenic variants in mitochondrial genes. In accordance with this possibility, a recent study on mitochondria-specific PRSs (mitoPRSs) demonstrated that combinations of small effect variants within genes regulating mitochondrial function were associated with higher PD risk.[14]

Herein, we extended the mitoPRS concept to subsets of genes controlling distinct mitochondrial pathways and demonstrated, in independent case–control datasets from 2 large, deeply phenotyped PD cohorts, that common variants in genes regulating OXPHOS were significantly associated with an increased risk of developing PD. Importantly, we functionally validated individual *OXPHOS*-PRS profiles in the corresponding patient-based cellular models, showing significant differences in mitochondrial respiratory function between iPD patients with high or low *OXPHOS*-PRS. iPD patients with high *OXPHOS*-PRS displayed a significantly earlier age at disease onset compared to those with low *OXPHOS*-PRS. Finally, patients with high *OXPHOS*-PRS responded more effectively to treatment with the mitochondrially active agent ursodeoxycholic acid (UDCA), suggesting that the *OXPHOS*-PRS may indeed allow for the selection of more homogenous PD patient groups for precision medicine in mitochondria-centred clinical trials.

Subjects and Methods

Study Design

Three studies were analyzed for this work. First, the exploratory dataset from the ongoing Luxembourg Parkinson's Study, a large longitudinal monocentric observational study in the framework

of the NCER-PD (National Centre for Excellence in Research in Parkinson's Disease) program comprising, at the time of data export, 493 PD patients and 625 healthy controls (HCs).[15] Second, the replication dataset from the COURAGE-PD (Comprehensive Unbiased Risk Factor Assessment for Genetics and Environment in Parkinson's Disease) consortium, including 21 sub-cohorts of European descent, but excluding samples from the Luxembourg Parkinson's Study and the International Parkinson's Disease Genomics Consortium (IPDGC) (7,422 PD patients and 6,904 HCs).[16,17] Third, an independent UK-based cohort (23 HCs and 55 iPD) pooling participants from 2 published studies: an observational study of multimodal mechanistic stratification of PD according to bioenergetic dysfunction and a clinical trial of UDCA in PD (i.e., the UP study, trial registration EudraCT no. 2018-001887-46).[18,19] Genotyping of the UP study cohort was undertaken at the Laboratory of Neurogenetics, NIH, Bethesda, Maryland, USA (Dr Sonja W. Scholz). All participants signed a written informed consent according to the Declaration of Helsinki. Ethical approval was granted by the National Committee for Ethics in Research, Luxembourg (Comité National d'Ethique de Recherche; CNER #201411/05). For UK-based studies, ethics were granted by the local Research Ethics Committees; REC 18/NW/0328 and REC 18/EE/0280.

Clinical Assessment

All participants in the Luxembourg Parkinson's Study underwent a comprehensive clinical assessment, as described elsewhere.[15] PD diagnosis was based on UKPDSBB criteria.[20] Clinical data reported here include the Movement Disorder Society update of the Unified Parkinson's Disease Rating Scale I (MDS-UPDRS I), MDS-UPDRS II, MDS-UPDRS III, MDS-UPDRS-IV, the Quality of Life questionnaire (PDQ39), the L-dopa-equivalent daily dose (LEDD), the Scales for Outcomes in Parkinson's Disease—Autonomic Dysfunction (SCOPA-AUT) and the Montreal Cognitive Assessment (MoCA). Age at onset (AAO) was defined as the age at PD diagnosis. Disease duration was defined as the number of years since the official PD diagnosis up to the time of data collection, i.e., up to the baseline visits for all individuals analyzed. All participants in the UP Study supplied an ethylenediaminetetraacetic acid (EDTA) blood sample for genetic analysis. The UP Study methodology and results have been described elsewhere.[18] As UDCA is a proposed mitochondrial rescue agent, phosphorus-31 magnetic resonance spectroscopy (31P-MRS) was used to assess target engagement within the midbrain. This allows the measurement of Gibbs free energy of ATP hydrolysis (ΔG_{ATP}), which reflects the useful energy released from the hydrolysis of ATP, therefore more negative values—as observed after 48 weeks treatment of UDCA compared to baseline—are possibly indicative of improved OXPHOS activity.[18]

Genotyping and Quality Control

DNA samples from participants in all cohorts were genotyped using the Neurochip array (v.1.0 and v1.1; Illumina, San Diego, CA) that was specifically designed to integrate neurodegenerative

disease-related variants.[21] Quality control (QC) of genotyping data was performed using PLINK v1.9,[22] as follows: samples with call rates <95% and whose genetically determined sex deviated from gender reported in the clinical data were excluded from the analysis, and the filtered variants were checked for cryptic relatedness and excess of heterozygosity. Samples exhibiting excess heterozygosity (F statistic > 0.2) and first-degree relatedness were excluded. After sample QC, SNVs with Hardy–Weinberg equilibrium p value < 1E-6, and missingness rates >5% were also excluded. QC was performed independently for each European cohort of the COURAGE-PD study, according to the standard procedures reported previously.[17] To focus our analysis on iPD cases, for both cohorts we also excluded carriers of pathogenic PD-associated variants in 8 PD-related genes (*ATP13A2*, *LRRK2*, *GBA*, *PARK7*, *PINK1*, *PRKN*, *VPS35*, and *SNCA*) identified *via* genotyping data.[23,24] For the Luxembourg Parkinson's Study, the presence of these mutations was confirmed by Sanger sequencing. To account for the population stratification, we calculated the first 3 principal components (PCs) using PLINK. The genotyping data were then imputed using the Haplotype Reference Consortium r1.1 2016 of the Michigan Imputation Server and filtered for imputation quality (R2 > 0.3).[25]

Mitochondrial Gene Sets and Pathway Resources

To assess the potential association between common variants in nuclear-encoded mitochondrial genes and PD risk, we first selected 3 different mitochondrial gene sets: Human MitoCarta3.0, which is a public inventory of 1,136 genes encoding proteins with putative mitochondrial localization,[26] and 2 gene sets previously reported by Billingsley and colleagues; the primary list (Billingsley I) contained 178 genes implicated in mitochondrial disorders, whereas the secondary list (Billingsley II) contained 1,327 genes regulating, more generally, mitochondrial function.[14]

Moreover, we defined 6 groups of genes—obtained from the Molecular Signatures Database (MsigDB) v7.5.1—known to participate in the following mitochondrial pathways potentially related to PD pathogenesis: *Mitochondrial DNA regulation*, *Mitophagy*, *Oxidative phosphorylation*, *TCA cycle*, *Mitochondrial protein import*, and *Mitochondrial proton transport* (Table S1).

Calculation of PRSs

Genome-wide PD-PRSs were calculated using the PRSice2 R package with default settings.[27] PRSs for each individual were generated by summing the weighted effects of the risk alleles (including all variants below the threshold for genome-wide significance) associated with PD—based on the largest PD GWAS summary statistics to date[4]—which are present in the 2 imputed target datasets (Luxembourg Parkinson's study and COURAGE-PD). PRSs for the general or pathway-specific mitochondrial gene sets (mitoPRSs) were generated using the PRSet function in PRSice2, using only risk alleles within gene regions outlined in the different gene lists. PRSice2 implement the clumping and thresholding (C + T) method. The criteria for linkage disequilibrium (LD) clumping of SNVs were pairwise LD r2 < 0.1 within a 250 kb window, ensuring that only independent genetic

variants contributed to the PRS. PRSs were computed at different p-value thresholds ranging from 5e-08 to 0.5. PRSice2 identified the optimal p-value threshold for variant selection that explained the maximum variance in the target sample. PRSice2 was also used to determine the observed phenotypic variance (PRS model fit, R2) explained by the genetic contribution of each mitochondrial pathways-PRS.

To control for the specificity of the contribution of PD GWAS risk alleles in predicting PD, we calculated the PRSs for the Luxembourg Parkinson's Study using SNVs from 3 base summary statistics of other disorders, namely type 2 diabetes, schizophrenia, and Alzheimer's disease (AD).[28–30]

Fibroblast Selection and Culture

Skin biopsies from the lower back region of study participants were collected in low-glucose Dulbecco's Modified Eagle Medium (DMEM, Thermo Fisher Scientific, #21885108) supplemented with 1% (v/v) penicillin–streptomycin (P/S, Thermo Fisher Scientific, #15140163). Each skin biopsy (5 mm diameter punch) was cut into multiple (up to 5) pieces and placed with the dermis facing down into a cell culture flask containing heat-inactivated Fetal Bovine Serum (HI-FBS, Thermo Fisher Scientific, #10270–106). After 10 minutes incubation at room temperature, DMEM containing 4.5 g/L glucose and 4 mM L-glutamine (Thermo Fisher Scientific, #41965039), supplemented with 10% (v/v) HI-FBS and 1% (v/v) P/S, was added to the flask, followed by incubation at 37°C in a 5% CO_2 humidified atmosphere. Cells were kept in the same medium for subsequent subculture, and subjected to Mycoplasma analysis on a regular basis to exclude potential contamination. Fibroblasts lines all had the same passage number at the time of the experiments, ranging from passage 5 to 10.

iPSC Generation

Fibroblast reprogramming into induced pluripotent stem cells (iPSCs) was performed by using the CytoTune™-iPS 2.0 Sendai Reprogramming kit (Thermo Fisher Scientific, #A16518), following the manufacturer's instructions (feeder-free conditions). Briefly, fibroblasts were transduced overnight with the reprogramming vectors hKOS, hc-Myc, and hKlf4, at MOI 5, 5, and 3, respectively, and then maintained in standard fibroblast medium until day 7 post-transduction. On day 7, fibroblasts under reprogramming were plated on Geltrex (Thermo Fisher Scientific, #A1413202)-coated wells, and switched to iPSCs medium starting from day 8. iPSCs medium consisted in DMEM-F12, Hepes (Thermo Fisher Scientific, #31330038), supplemented with 1% P/S, 1% insulin-transferrin-selenium (ITS-G, Thermo Fisher Scientific, #41400045), 64 μG/mL L-ascorbic acid 2-phosphate magnesium (Sigma, #A8960), 100 ng/ml heparin (Sigma, #H3149-25KU), 2 ng/ml transforming growth factor beta-1 (TGF-β1) (Peprotech, #100–21), and 10 ng/ml fibroblasts growth factor (FGF)-basic (Peprotech, #100-18B). Between day 21 and 28 post-transduction, undifferentiated iPSC colonies were manually transferred into Geltrex-coated 12-well plates for further expansion and characterization.

Generation and Maintenance of Neuronal Progenitor Cells

The procedure for obtaining neuronal progenitor cells from iPSCs was described previously. Their identity is restricted to both midbrain and hindbrain fates, whereas they are unable to form forebrain neurons.[31] Briefly, iPSCs were shifted to N2B27 medium—consisting of 49% DMEM/F12 (Thermo Fisher Scientific, #21331020), 49% Neurobasal (Thermo Fisher Scientific, #21103049), 1:100 B27 supplement without vitamin A (Thermo Fisher Scientific, #12587010), 1:200 N2 supplement (Thermo Fisher Scientific, #17502001), 1% (v/v) Glutamax (Thermo Fisher Scientific, #35050061) and 1% (v/v) P/S—supplemented with 10 μM SB-431542 (R&D Systems, #1614/10), 1 μM Dorsomorphin (R&D Systems, #3093), 3 μM CHIR 99021 (CHIR, Axon Medchem, #2435) and 0.5 μM purmorphamine (PMA, Sigma, #SML0868). After 4 days in this medium, SB-431542 and Dorsomorphin were removed and cells maintained in N2B27 medium containing CHIR, PMA, and 150 μM ascorbic acid (AA, Sigma, #A4403). On day 5, the emerging neural epithelium was isolated, triturated into smaller pieces and plated on Geltrex-coated wells. The resulting neuronal progenitor cells (smNPCs) were further expanded in N2B27 medium supplemented with CHIR, PMA and AA.

The smNPCs from 2 PD patients carrying the c.1366C > T mutation in the *PINK1* gene (p.Q456X) were described previously.[32]

Analysis of Mitochondrial Respiration

Oxygen consumption rates (OCRs) were determined by using the Seahorse XFe96 FluxPak (Agilent, #102416–100) and XF Cell Mito Stress Test (Agilent, #103015–100) kits, in accordance with the manufacturer's instructions. For primary skin fibroblasts, 5,000 cells per well were seeded in a 96-well Seahorse cell culture plate (at least 5 technical replicates per line) and incubated overnight. The following day, fibroblast medium in each well was replaced with 175 μl Seahorse XF DMEM medium pH 7.4 (Agilent, #103575–100), supplemented with 25 mM glucose, 2 mM L-glutamine and 1 mM sodium pyruvate, followed by 1 h incubation at 37°C without CO_2. In the meantime, the sensor cartridge—previously equilibrated overnight in the XF Calibrant solution at 37°C without CO_2—was loaded with standard mitochondrial toxins, namely Oligomycin (1 μM final concentration in the assay well), carbonyl cyanide p-trifluoromethoxyphenylhydrazone (FCCP, 0.6 μM final concentration in the assay well) and a mixture of Rotenone and Antimycin A (both at the concentration of 0.5 μM in the assay well). After an additional incubation at 37°C without CO_2 for 30 minutes, the sensor cartridge, as well as the cell culture plate, were loaded on the XFe96 Extracellular flux Analyzer (Agilent). Three OCR measurements were performed for both basal respiration and after each automated injection of mitochondrial toxins. OCR data were analyzed using the XFe Wave software (Agilent) and exported using the Seahorse XF Cell Mito Stress Test Report Generator. Initial OCR values as well as OCR measurements after each injection step were used to calculate different parameters related to oxidative phosphorylation, including

basal respiration, proton leakage across the inner mitochondrial membrane, respiration coupled to ATP synthesis, maximal respiration, and spare respiratory capacity.[33]

Seahorse experiments in neuronal progenitor cells were performed in Neurobasal medium containing either glucose or galactose as carbon source.[34] Briefly, 35,000 cells per well were first seeded in a Geltrex-coated 96-well Seahorse cell culture plate (at least 10 replicates per line), in 100 μl N2B27 medium containing CHIR, PMA and AA. The day after, N2B27 medium was removed and replaced by Neurobasal-A without glucose and sodium pyruvate (Thermo Fisher Scientific, #A2477501), then supplemented with 0.727 mM sodium pyruvate and either 25 mM glucose or 25 mM galactose. Similar to the standard N2B27 used for maintenance of neuronal progenitor cells, this medium also contained N2, B27 and glutamax supplements, 1% (v/v) P/S, as well as CHIR, PMA, and AA. Neuronal progenitor cells remained in glucose- or galactose-based media for 48 hours before proceeding with the Seahorse protocol described above. Either glucose or galactose (always 25 mM) were also added to the Seahorse assay medium (XF DMEM pH 7.4) used during the entire procedure.

OCR data were normalized against protein (fibroblasts) or DNA (smNPCs) content, as defined by the PIERCE™ BCA protein assay kit (Thermo Fisher Scientific, #23225) or the CyQUANT cell proliferation assay kit (Thermo Fisher Scientific, #C7026), respectively.

Statistical Analysis

The predictive accuracy of the PRS model was determined using the area under the receiver operating curve (AUC, pROC R package). A higher AUC indicates a better PRS model able to discriminate between PD cases and controls. We compared the PRS distribution in HC vs iPD subjects using the non-parametric Wilcoxon rank-sum test, as the data did not display a normal distribution. To further investigate whether the PRSs could predict PD risk, a logistic regression model was used to calculate the odds ratio (OR). OR is always given with confidence interval. Gender, age at assessment, and the first 3 PCs from the population stratification were included as covariates.

Individuals were stratified into 3 groups based on *OXPHOS*-PRS percentiles: low (<10%), intermediate (10–90%), and high (>90%). Comparison of PD-specific clinical outcomes, AAO, and disease duration between individuals in the high and low *OXPHOS*-PRS groups was performed using the Welch's t-test. Statistical analyses were done in R (v4.0.4). To account for multiple hypothesis testing and reduce the risk of type I errors, we applied the false discovery rate (FDR) correction using the Benjamini-Hochberg method, with an adjusted p-value threshold of <0.05 deemed to be significant. For the functional assays (all involving more than 2 groups), statistical significance was assessed using 1-way ANOVA, after confirming normality of the data using a Shapiro–Wilk test. For experiments with 2 independent variables, 2-way ANOVA was used considering interaction effects. In both cases, Tukey's post hoc correction for multiple comparisons was applied after the ANOVA tests. Statistical analyses of functional data were performed using the GraphPad Prism software (v9.4.0). Data with error bars are represented as mean ± SEM and are representative of at least 3 independent biological replicates. Two-way ANOVA combining treatment group and PRS risk groups with an interaction effect was used to assess for differential treatment responses between these groups in clinical parameters from The UP Study. Any significant ANOVA underwent post-hoc analysis using Tukey's test.

Results

Association of Common Variants in Mitochondrial Genes with PD Risk

To gain essential knowledge about the mitochondria-related "missing heritability" in iPD, we analyzed the distribution of mitoPRSs in 2 distinct case–control datasets, namely the Luxembourg Parkinson's Study[15] and COURAGE-PD[16,17] cohorts. After filtering and QC, the final dataset for the Luxembourg Parkinson's Study comprised 412 iPD patients and 576 HC. iPD patients were older than the HC (67.5 ± 10.9 *vs* 59.1 ± 12.2 years, p-value < 0.01) with a mean AAO of 62.2 ± 11.8 years and a mean disease duration of 5.4 ± 5.0 years (Table).

TABLE. Demographic Data of iPD Patients and Healthy Controls (HCs) from the Luxembourg Parkinson's Study and COURAGE-PD cohorts

Parameter	Luxembourg Parkinson's Study		COURAGE-PD	
	iPD	HCs	iPD	HCs
n	412	576	7,270	6,819
Age at assessment (years, mean ± SD)	67.5 ± 10.9	59.1 ± 12.2	67.4 ± 11.2	66.4 ± 11.8
Age at onset (years, mean ± SD)	62.2 ± 11.8	-	58.7 ± 11.6	-
Disease duration (years, mean ± SD)	5.4 ± 5.0	-	8.6 ± 6.5	-
Sex (% male/female)	67.9/32.1	56.9/43.1	60.1/39.9	45.3/54.7

Note: Means and percentages were calculated after filtering and quality controls of genotyping data.

Using the PD GWAS summary statistics reported by Nalls and colleagues,[4] we first calculated the genome-wide PRS for the Luxembourg Parkinson's Study and found a significant association with PD compared to HC (OR = 1.57 [1.36–1.82]; FDR-adj p-value = 8e-09, AUC = 0.62, Fig 1A). To capture the cumulative effect of common variants in nuclear-encoded mitochondrial genes on PD risk, we then selected 3 general mitochondrial gene-sets: Human MitoCarta 3.0,[26] and 2 additional gene lists previously used by Billingsley and colleagues.[14] Strikingly, all 3 mitochondrial gene-sets were significantly associated with PD (FDR-adj p-value < 0.05, Fig 1B): (i) Billingsley I (OR = 1.18[1.02–1.35]), (ii) Billingsley II (OR = 1.26 [1.09–1.46]), and (iii) MitoCarta 3.0 (OR = 1.24[1.08–1.44]). Next, we applied the same approach to different mitochondrial pathways, aimed at obtaining PRSs related to specific mitochondrial alterations possibly involved in PD pathogenesis. We, therefore, selected 6 potentially relevant mitochondrial pathways, containing groups of genes annotated in the corresponding Molecular Signatures Database (MsigDB) sub-collections (Table S1), and calculated mitochondria-specific PRSs. The degree of overlap between the different mitochondrial gene-sets is presented

in Fig S1. As shown in Fig 1C, only variants in the *OXPHOS* gene set were significantly associated with a higher PD risk in the Luxembourg Parkinson's Study (OR = 1.31[1.14–1.50], FDR-adj p-value = 5.4e-04). To assess genetic risk without considering the potential contribution of variants in known PD loci included in the *OXPHOS* gene list (i.e., *PINK1*, *SNCA* and *PARK7*, as defined by the MDS gene classification list for PD, https://www.mdsgene.org), we performed the PRS analysis for the significant *OXPHOS* pathway after the exclusion of these genes. In this setting, the OR was slightly reduced (OR = 1.24[1.08–1.43], FDR-adj p-value = 5.3e-03), but the association with PD risk remained significant (Fig 1D). To take into account SNVs in potential gene regulatory elements, we have also calculated pathway-specific mitoPRSs after extending boundaries upstream (35 kb) and downstream (10 kb) of each gene.[35] Similar results as before were observed, except for the Billingsley I gene set that was no longer significant (OR = 1.15[1.00–1.32], FDR-adj p-value = 0.08). The other mitochondrial gene-sets were still significantly associated with PD: Billingsley II (OR = 1.21[1.05–1.39], FDR-adj p-value = 1.4e-02), MitoCarta3.0 (OR = 1.27[1.10–1.46],
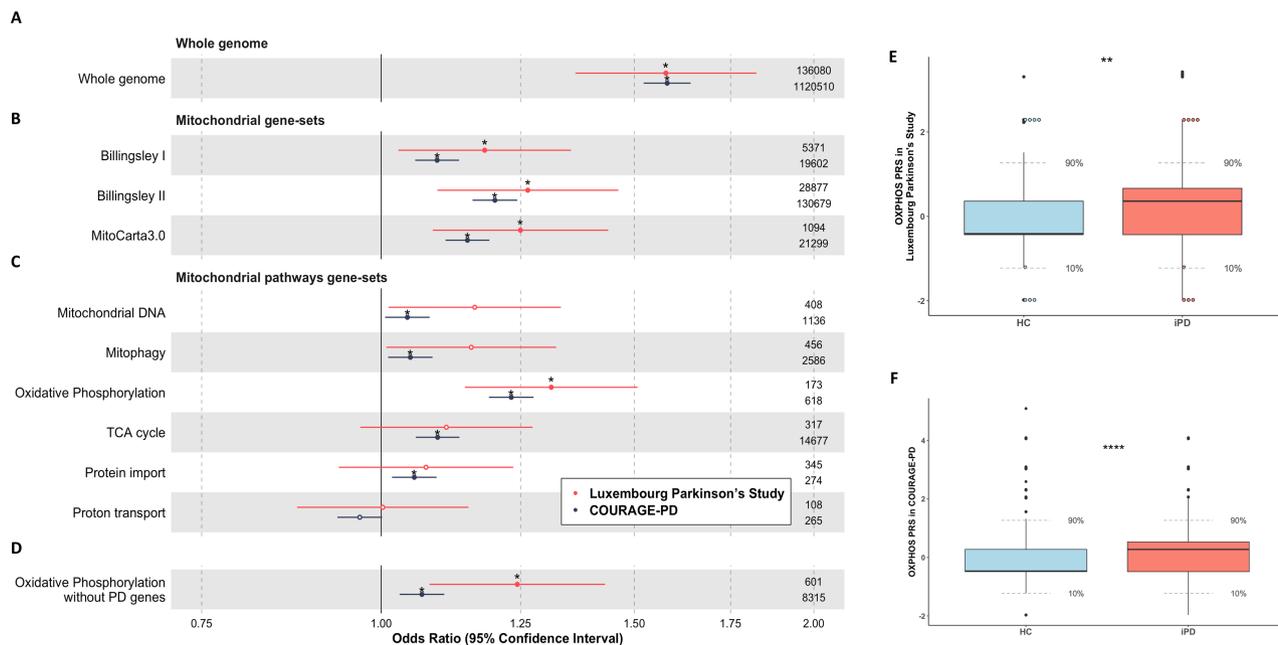
FIGURE 1: Common variants in mitochondrial genes are associated with higher PD risk. (A–D) Forest plots of the odds ratio (OR) and 95% confidence interval for the whole genome (A), 3 different mitochondrial gene sets (B), and 6 selected mitochondrial pathways (C) polygenic risk scores (PRSs) regressed with PD diagnosis in the Luxembourg Parkinson's Study (in red) and COURAGE-PD (in dark blue) cohorts. (D) OR for the significant *OXPHOS* pathway was also plotted upon removal of PD-related genes (i.e., *PINK1*, *SNCA*, and *PARK7*) from the *OXPHOS* gene list. Only significant FDR-adjusted p-values are shown on top of each point (* p-value < 0.05). The number of SNVs used to calculate each PRS is shown on the right side. (E, F) Distribution of standardized *OXPHOS*-PRS in iPD patients (iPD, *red*) and healthy controls (HCs, *light blue*) from the Luxembourg Parkinson's Study (E) and COURAGE-PD (F) cohorts. The PRS distribution between iPD and HC was significantly different in both datasets (** Wilcoxon test p-value < 0.01; **** Wilcoxon test p-value < 0.0001). Colored dots in E indicate PRS values of iPD cases and HC in the highest and lowest *OXPHOS*-PRS range (10th and 90th percentile, n = 4 for each group) whose primary skin fibroblasts were available for functional studies.

FDR-adj p-value = 2.5e-03), as well as *OXPHOS* (OR = 1.33[1.16–1.53], FDR-adj p-value = 2.7e-04) (Fig S2). Of note, using common risk alleles associated with other diseases (i.e., type 2 diabetes, schizophrenia, and AD GWAS summary statistics)[28–30] for the calculation of mitoPRSs in the imputed Luxembourg Parkinson's Study cohort, we found that none of them were significantly associated with an increased PD risk (Fig S3), thus confirming the specificity of our findings based on common PD GWAS SNVs.

Next, we used the 21 sub-cohorts of the COURAGE-PD consortium (Table S2)[16,17] as a larger replication dataset to validate the results obtained in the exploratory Luxembourg Parkinson's Study. After filtering and QC, the COURAGE-PD dataset comprised 7,270 iPD cases and 6,819 HCs. The demographic features of COURAGE-PD are shown in Table. The genome-wide PRS as well as all tested mitoPRSs, including *OXPHOS*-PRS (OR = 1.23[1.18–1.27], FDR-adj p-value = 1.5e-29), were significantly associated with PD risk in COURAGE-PD (Fig 1A–D). Again, *OXPHOS*-PRS remained significantly associated with PD risk when the PD-related genes *PINK1*, *SNCA*, and *PARK7* were excluded from the *OXPHOS* gene list (OR = 1.06[1.02–1.10], FDR-adj p-value = 5.6e-04) (Fig 1D).

We also assessed the phenotypic variance and the predictive accuracy of each mitoPRS model, using the R2 metric and AUC analysis, respectively. Strikingly, among the tested mitochondrial pathways, only the *OXPHOS*-PRS model significantly predicted PD status in both, the Luxembourg Parkinson's study (R2 = 0.015, FDR-adj p-value = 0.003; AUC = 0.56) and COURAGE-PD (R2 = 0.010, FDR-adj p-value = 3.4e-33; AUC = 0.56) cohorts (Fig S4 and Table S3). Finally, to correct for imbalance in the case–control ratio, we have also measured the phenotypic variance after adjusting for an estimated PD prevalence of 0.005.[36] The resulting adjusted R2 (R2*) for the *OXPHOS*-PRS model was still the highest score among the tested pathways in both, the Luxembourg Parkinson's study (R2* = 0.0058) and COURAGE-PD (R2* = 0.00366) cohorts (Table S3).

The PRS distribution between iPD and HCs was significantly different both in the Luxembourg Parkinson's Study (Wilcoxon test p-value = 1.4e-03, Fig 1E) and in the COURAGE-PD cohorts (Wilcoxon test p-value = 2.2e-16, Fig 1F).

To determine whether the *OXPHOS*-PRS could represent a pathophysiology relevant tool to stratify iPD patients based on mitochondrial dysfunction, we sought to functionally validate the predicted phenotypes in patient-derived cellular models. Participants were grouped into low-, intermediate-, or high-risk groups according to the PRS distribution in the lower and higher deciles.[37,38] Decile cutoffs of 10% and 90%, corresponding to the lowest and highest PD ORs, were chosen for the subsequent functional studies (Fig S5). Thus, iPD patients with the highest or lowest *OXPHOS*-PRSs (10th and 90th percentile, respectively) were identified among the Luxembourg Parkinson's Study participants and available primary skin fibroblasts from these individuals (at least n = 4 from each group) were used in functional experiments. In parallel, fibroblasts from HCs with extreme *OXPHOS*-PRS values (10th and 90th percentile, at least n = 4 for each group) were selected as reference for the comprehensive mitochondrial phenotyping performed in cells from iPD patients (Fig 1E and Table S4).

Mitochondrial Oxygen Consumption Is Significantly Elevated in Primary Skin Fibroblasts from iPD Patients with High OXPHOS-PRS

To functionally validate the association between *OXPHOS*-PRS and PD risk in patient-derived cells, we first assessed mitochondrial respiratory chain performance using the Seahorse technology, which provides a comprehensive overview of mitochondrial bioenergetics by measuring oxygen consumption rates (OCRs) under basal conditions and after targeted inhibition of specific respiratory chain complexes.[33] Strikingly, basal and ATP-linked respiration were significantly enhanced in fibroblasts from iPD patients with high *OXPHOS*-PRS compared to low *OXPHOS*-PRS cells (Fig 2). In this setting, maximal respiration was not significantly different between high and low *OXPHOS*-PRS iPD fibroblasts, indicating a reduced spare respiratory capacity in the high *OXPHOS*-PRS iPD group. Of note, all respiratory parameters analyzed were not significantly different between HCs with high or low *OXPHOS*-PRS (Fig 2). Similarly, biogenesis of respiratory chain complexes (RCC) did not differ significantly between the high and low *OXPHOS*-PRS groups—both in HCs and in iPD patients—as revealed by immunoblot analysis of RCC protein subunits (Fig S6). Taken together, these results suggest that fibroblasts from iPD patients with high *OXPHOS*-PRS display features of mitochondrial hyperactivity even under steady-state conditions, a phenotype that appears to be independent of RCC protein expression.

Other Functional Readouts of Mitochondrial Activity Are Not Significantly Altered in Fibroblasts from iPD Patients Stratified Based on OXPHOS-PRS

To assess whether changes in mitochondrial respiration were accompanied by differences in reactive oxygen species (ROS) production, fibroblasts from both iPD patients and HCs stratified according to their individual *OXPHOS*-PRS
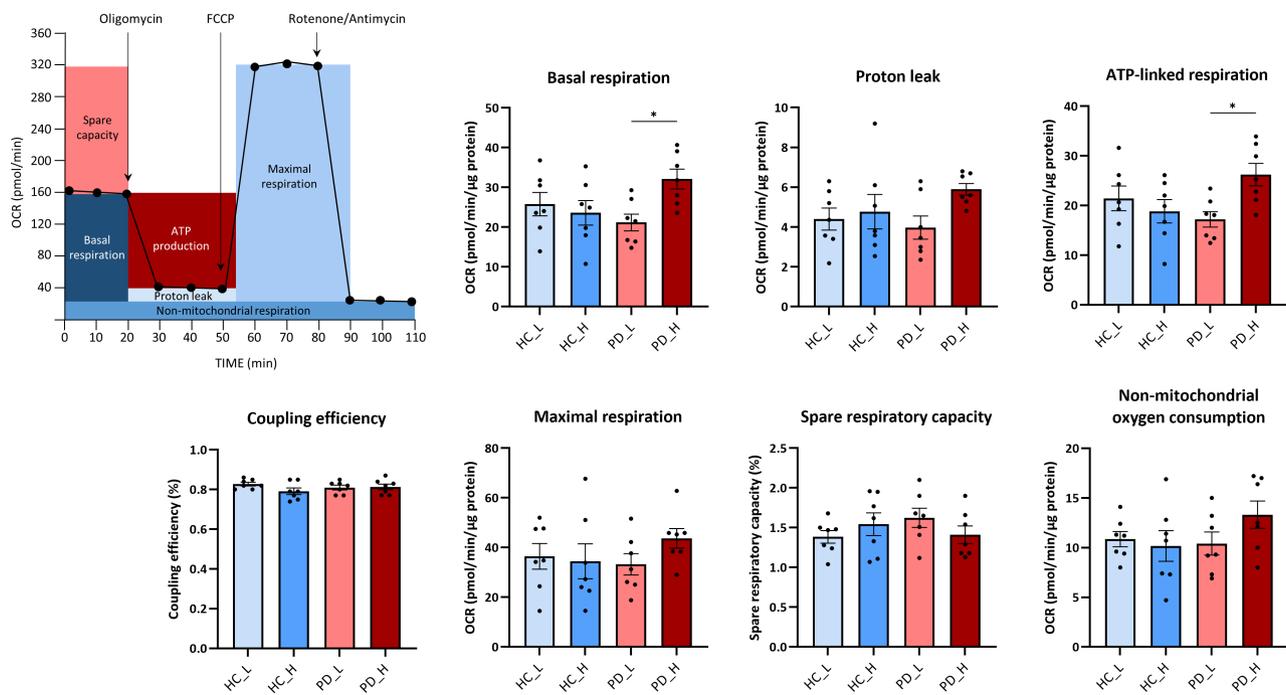
FIGURE 2: Analysis of mitochondrial respiration in primary skin fibroblasts from iPD patients and HCs stratified based on *OXPHOS*-PRS. Oxygen consumption rates (OCRs) were measured under basal conditions and after targeted inhibition of specific respiratory chain complexes by using a standard Seahorse Mito Stress test. Histobars represent the mean ± SEM of 7 fibroblast lines per group established from the Luxembourg Parkinson's Study participants (HCs vs iPD patients) with high (HC_H; PD_H) or low (HC_L; PD_L) *OXPHOS*-PRS. For each cell line, at least 3 independent experiments were performed. At least 5 technical replicates per group (i.e., distinct Seahorse wells) were analyzed in each experiment. One-way ANOVA correcting for multiple comparisons using the Tukey's post hoc test. *p-value < 0.05.

were subjected to CellROX staining. Surprisingly, increased ROS levels were detected in HCs from the high *OXPHOS*-PRS group compared to both low-risk HC and iPD patients, arguing against a causal link between elevated OXPHOS and ROS accumulation in these cells (Fig 3A). Given the important role of the electrochemical gradient across the inner mitochondrial membrane in generating the proton motive force used by the OXPHOS machinery to synthesize ATP,[39] we also measured mitochondrial membrane potential ($\Delta\Psi_m$) in primary skin fibroblasts from each *OXPHOS*-PRS group. To this end, cell lines were stained with tetramethylrhodamine ethyl ester (TMRE), a fluorescent dye that specifically accumulates in active, polarized mitochondria, followed by high-throughput automated confocal microscopy analysis. Treatment with the OXPHOS uncoupler carbonyl cyanide 3-chlorophenylhydrazone (CCCP), known to induce mitochondrial depolarization, was used as a positive control for decreased $\Delta\Psi_m$. As expected, CCCP-treated cells all failed to accumulate the dye within mitochondria and, therefore, displayed a robust reduction of TMRE fluorescence. However, no significant differences in $\Delta\Psi_m$ were observed between untreated fibroblasts from both HCs and iPD patients previously stratified according to their low or high *OXPHOS*-PRS (Fig 3B). OXPHOS can also be affected by abnormal mitochondrial

fission/fusion processes, as revealed by changes in ETC activity and respiratory function in response to dynamic transitions of organelle morphology—from fragmented to elongated, and vice versa.[40,41] Again, we observed no difference in morphological parameters such as mitochondrial *aspect ratio* and *form factor* in fibroblasts derived from HCs and iPD patients with high or low *OXPHOS*-PRS (Fig 3C). mtDNA copy number, transcription/replication rates and deletions, which could impinge on ETC activity by altering the expression and stoichiometric assembly of mtDNA-encoded RCC subunits,[12,42,43] were also not significantly different between the high and low *OXPHOS*-PRS groups (Fig S7). Finally, based on the emerging link between mitochondrial dysfunction and inflammation in PD,[44,45] we measured interleukin-6 (IL-6) levels in blood plasma samples from the Luxembourg Parkinson's Study participants (both HCs and iPD patients) with the highest or lowest *OXPHOS*-PRS. Indeed, we recently found increased IL-6 levels in the serum of PD patients carrying biallelic rare variants in *PINK1* or *PRKN*,[44] a phenotype mainly associated with impaired mitophagy and dependent on activation of the pro-inflammatory cGAS-STING pathway.[45] Here, we did not observe significant differences in plasma IL-6 levels between the high and low *OXPHOS*-PRS groups (Fig 3D).
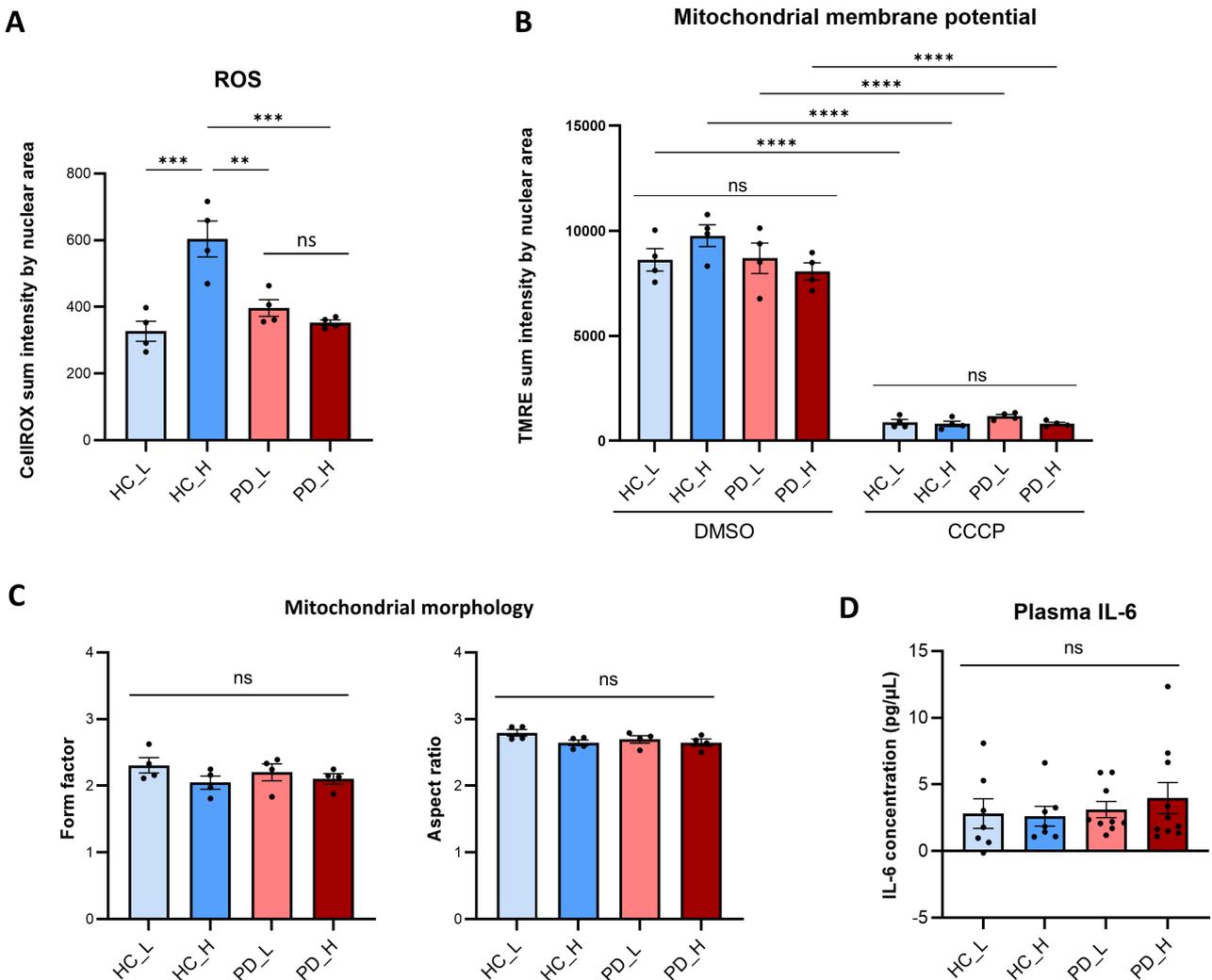
FIGURE 3: Assessment of additional readouts of mitochondrial activity in primary skin fibroblasts and plasma samples from iPD patients and HCs stratified based on *OXPHOS*-PRS. (A–C) High-throughput confocal microscopy analyses in primary skin fibroblasts derived from Luxembourg Parkinson's Study participants with high (HC_H; PD_H) or low (HC_L; PD_L) *OXPHOS*-PRS. (A) ROS levels were quantified by normalizing the CellRox mean fluorescence intensity against the nuclear area, as defined by the Hoechst staining. Histobars represent the mean $\pm$ SEM of 4 distinct fibroblast lines per group. Three independent experiments were performed for each line. One-way ANOVA correcting for multiple comparisons using the Tukey's post hoc test. **p-value < 0.01; *** p-value < 0.001. ns = not significant. (B) Mitochondrial membrane potential ($\Delta\Psi_m$) was measured after normalization of TMRE mean fluorescence intensity by the nuclear area. Treatment with the OXPHOS uncoupler carbonyl cyanide 3-chlorophenylhydrazone (CCCP), known to induce mitochondrial depolarization, was used as positive control for decreased $\Delta\Psi_m$. Dimethyl sulfoxide (DMSO) was used as a vehicle. Histobars represent the mean $\pm$ SEM of 4 distinct fibroblast lines per group. At least 3 independent experiments were performed for each line. Two-way ANOVA correcting for multiple comparisons using the Tukey's post hoc test. ****p-value < 0.0001. ns = not significant. (C) Morphometric analysis of the mitochondrial network. *Form factor* and *aspect ratio* were quantified as described previously.[71] Histobars represent the mean $\pm$ SEM of 4 distinct fibroblast lines for each group. At least 3 independent experiments were performed for each line. One-way ANOVA correcting for multiple comparisons using the Tukey's post hoc test. ns = not significant. (D) Measurement of IL-6 levels in plasma samples obtained from Luxembourg Parkinson's Study participants (HCs vs iPD patients) with high (HC_H, n = 7; PD_H, n = 10) or low (HC_L, n = 7; PD_L, n = 9) *OXPHOS*-PRS. Brown-Forsythe and Welch ANOVA correcting for multiple comparisons using Dunnett's T3 test. ns = not significant.

Functional Validation of OXPHOS-PRS in iPSC-Derived Neuronal Progenitors

To validate our *OXPHOS*-PRS approach in more disease-relevant patient-derived models, we reprogrammed fibroblast lines from both HCs and iPD patients with high or low *OXPHOS*-PRS into induced

pluripotent stem cells (iPSCs). We successfully reprogrammed 7 HC (3 low-risk and 4 high-risk) and 11 iPD (5 low-risk and 6 high-risk) lines. The newly generated iPSCs all showed no chromosomal aberrations and an identical genetic background compared to the original skin fibroblasts (Fig S8A,B). Different from

fibroblasts, iPSCs all expressed high RNA levels of the stemness markers *OCT3/4* and *NANOG* (Fig S8C). Next, iPSC lines were differentiated into smNPCs,[31] and then subjected to an assessment of mitochondrial respiration. Seahorse-based bioenergetics analyses in smNPCs did not reveal major differences in OCRs between the low and high OXPHOS-PRS groups (Fig 4), likely due to their high glycolytic activity and low reliance on OXPHOS metabolism.[46] In accordance with this hypothesis, shifting smNPCs from glucose to galactose medium as carbon source dramatically increased basal and ATP-linked respiration, indicative of a metabolic switch from glycolysis to OXPHOS (Fig 4). In this setting, smNPCs derived from iPD patients with high *OXPHOS*-PRSs displayed a significant decrease of basal respiration, proton leak, and ATP-linked respiration compared to the low *OXPHOS*-PRSs group, comparable to that observed in smNPCs from patients with autosomal recessive PD caused by rare variants in the *PINK1* gene. Notably, OCR values did not significantly vary between HCs with high or low *OXPHOS*-PRS, both in glucose and in galactose media (Fig 4).

Association of OXPHOS-PRSs with PD-Specific Clinical Outcomes

We sought to investigate whether our functionally validated *OXPHOS*-PRS approach could be used to define distinct phenotypic patterns among iPD patients. To this end, we first analyzed 8 PD-specific motor and non-motor clinical scores in iPD patients from the Luxembourg Parkinson's Study stratified according to their *OXPHOS*-PRS, namely the Movement Disorder Society update of the Unified Parkinson's Disease Rating Scale I (MDS-UPDRS I), MDS-UPDRS II, MDS-UPDRS III, MDS-UPDRS-IV, the Quality of Life questionnaire (PDQ39), the L-dopa-equivalent daily dose (LEDD), the Scales for Outcomes in Parkinson's Disease—Autonomic Dysfunction (SCOPA-AUT), and the Montreal Cognitive Assessment (MoCA). The whole-genome PRS was used as reference. In general, the trend of all clinical outcomes analyzed was similar to that observed for the whole-genome PRS, and none of them was significantly different between iPD patients with high or low *OXPHOS*-PRS (Fig S9). However, iPD patients with high *OXPHOS*-PRS had an earlier AAO compared to low-risk patients, a phenotype that was particularly evident in the larger

FIGURE 4: Functional validation of *OXPHOS-PRS* in iPSC-derived neuronal progenitors. Oxygen consumption rates (OCRs) were measured under basal conditions and after targeted inhibition of specific respiratory chain complexes by using a standard Seahorse Mito Stress test. Histobars represent the mean ± SEM of 3 (HC_L), 4 (HC_H), 5 (PD_L), 6 (PD_H) and 2 (PD_PINK1) distinct smNPC lines per group, cultivated either in glucose or galactose medium. At least 3 independent experiments were performed for each line. At least 6 technical replicates per group (i.e., distinct Seahorse wells) were analyzed in each experiment. Two-way ANOVA correcting for multiple comparisons using the Tukey's post hoc test. *p-value < 0.05; **p-value < 0.01; ***p-value < 0.001; ****p-value < 0.0001.

COURAGE-PD dataset (FDR-adj p-value = 0.015, Fig 5A,B). In accordance with this, the *OXPHOS*-PRS negatively correlated with AAO in the Luxembourg Parkinson's Study (Spearman correlation $r = -0.16$, p-value = 0.001, Fig S10).

Finally, as an exploratory analysis we wanted to investigate if our approach using *OXPHOS*-PRS for patient stratification could allow the identification of PD patients that are more responsive to drugs targeting mitochondria. To this end, participants of the "UP Study" with genetic data available were retrospectively stratified according to the same *OXPHOS*-PRS strategy, applied to the entire UK cohort separately. Risk classification was based on quartiles; within each group (iPD or HCs), individuals with PRS values within the highest quartile were assigned to 'high' risk, those in the lowest quartile to
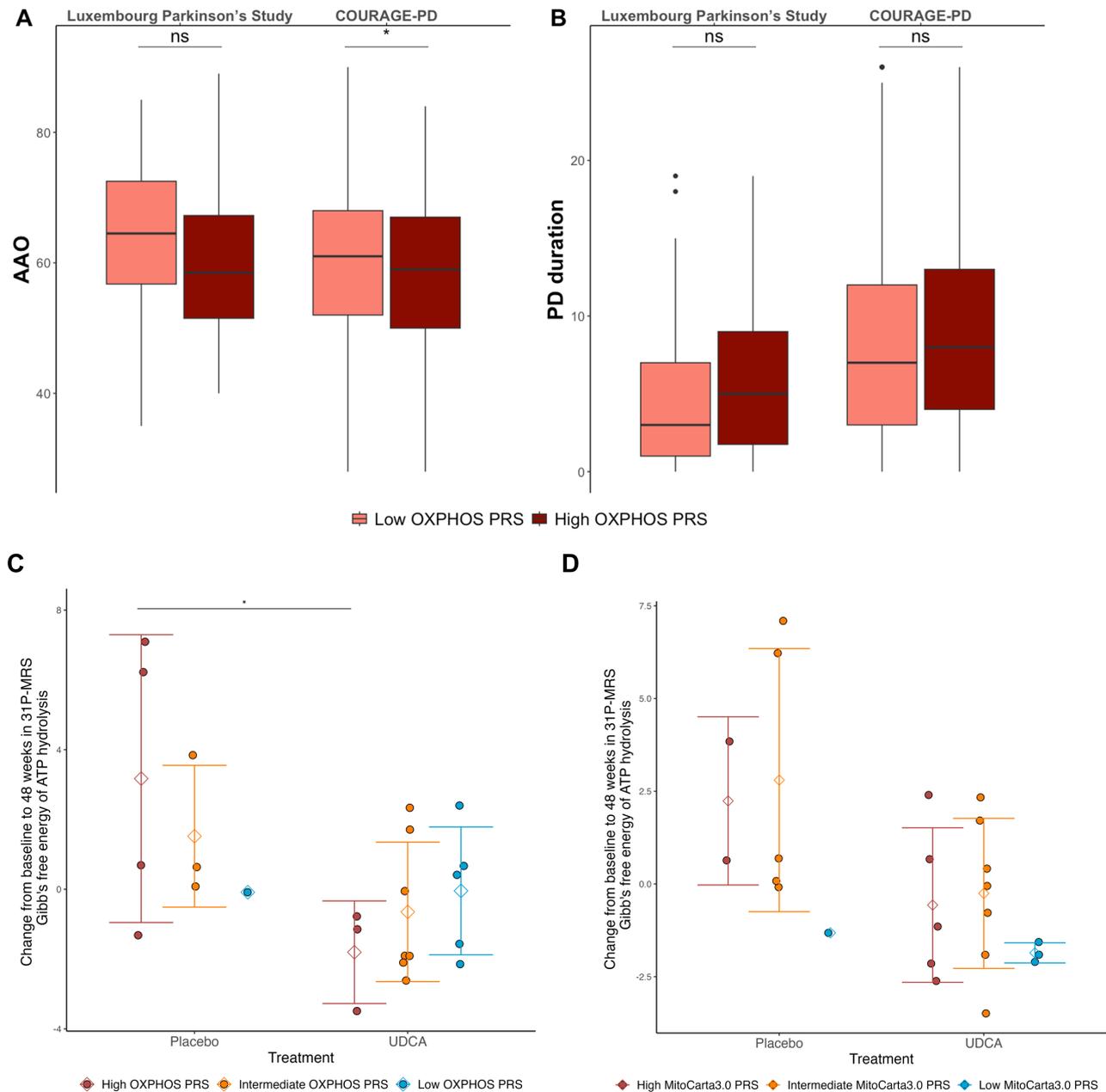
FIGURE 5: Association of *OXPHOS*-PRSs with age at PD onset and disease duration. (A, B) Comparison of mean age at PD onset (AAO, A) and mean disease duration (B) in iPD patients from the Luxembourg Parkinson's Study and COURAGE-PD cohorts with high or low *OXPHOS*-PRS. *p-value < 0.05, ns = not significant. **(C, D)** Changes in Gibbs free energy of ATP hydrolysis (ΔG_{ATP}) in UP Study PD patients treated with UDCA or placebo for 48 weeks. Mean (*diamond*) and standard deviation (*error bars*) are shown for high- (*red*), intermediate- (*orange*), or low- (*blue*) PRS groups stratified according to *OXPHOS*-PRS (C) or MitoCarta-PRS (D). Two-way ANOVA considering treatment effect and interaction between treatment and PRS groups, followed by post-hoc pairwise t-test between significant comparison groups using Tukey's correction. *p-value < 0.05.

'low' and the remainder being assigned 'intermediate'. Although less stringent, quartile-based classification was necessary to ensure sufficient numbers of participants within each risk group to enable this exploratory analysis. As previously shown,[18] the UDCA treatment group had an overall improvement in the Gibbs free energy of ATP hydrolysis compared to the placebo group ($\Delta G_{ATP} = -2.82$, 95% CI -4.78, -0.86, p-value = 0.0074). There was a significant interaction between UDCA treatment and the *OXPHOS*-PRS risk group (p-value = 0.04824). This treatment effect was significantly greater within the high *OXPHOS*-PRS groups taking UDCA compared to the high *OXPHOS*-PRS group on placebo ($\Delta G_{ATP} = -6.47$, 95% CI -12.02, -0.93, p-value = 0.0172, Fig 5C). Of note, no significant differences were observed upon patients' stratification according to the general MitoCarta-PRS apart from the expected global treatment effect (Fig 5D).

Discussion

Despite recent advances in the generation and analysis of large-scale genotyping data, unravelling the complex genetic architecture of PD remains still a major challenge. Low-penetrance genetic variants that significantly increase the risk of developing PD have been identified in sporadic cases (e.g., *GBA* L444P and *LRRK2* G2019S), but typical hallmarks of PD heritability can also be observed in families with unknown genetic causes,[47] which suggests a potential involvement of genetic factors in up to 30% of identified PD cases.[48]

Missing heritability in PD and the clear association between mitochondrial dyshomeostasis and neurodegeneration led us to investigate the role of disease-associated SNVs in genes regulating mitochondrial function. Thus, we performed association analyses targeting common variants in nuclear-encoded mitochondrial genes and analyzed the mitoPRS distribution in 2 distinct iPD case–control studies, namely the Luxembourg Parkinson's Study and the COURAGE-PD consortium. After testing several common mitochondrial gene-sets, we found that mitoPRSs were always significantly associated with increased PD risk in both cohorts. Of note, PRSs can also be applied to subsets of genes that control distinct, disease-related cellular activities (e.g., mitochondrial quality control or lysosomal function in PD), aimed at identifying specific pathways implicated in the pathological phenotype.[36] Using this approach, Paliwal and colleagues recently demonstrated that certain mitochondrial pathways—including *OXPHOS* among others—were significantly associated with increased AD risk.[49] In a similar manner, here, we used gene lists for 6 mitochondrial pathways relevant to PD and calculated pathway-specific mitoPRSs. Strikingly, only common variants in genes regulating *OXPHOS* were significantly associated with increased PD risk in the Luxembourg Parkinson's Study and COURAGE-PD cohorts, reinforcing the notion of impaired mitochondrial respiration as a relevant aspect in PD pathogenesis.

PRS-based approaches appear to be increasingly useful for dissecting genetically heterogeneous disorders and identifying pathophysiology-relevant disease subtypes.[50–52] However, to date, only 3 studies used PRS-based approaches to assess mitochondrial risk in PD.[14,36,53] Two of them demonstrated that a combination of small effect-size common variants in nuclear-encoded mitochondrial genes was significantly associated with higher PD risk,[14,54] while the other one failed to confirm this association but showed functional enrichment of mitochondria-related pathways—including OXPHOS.[36] One study also demonstrated an association between mitoPRSs and clinical outcomes.[53] However, none of these studies considered the need to functionally validate PRSs in patient-based cellular models, which would legitimize the effectiveness of genetically predicted cellular phenotypes thus paving the way for precision medicine therapeutic approaches.[54] In addition, there have been attempts to stratify iPD patients exclusively based on mitochondrial phenotyping assays.[55] However, this type of stratification is time-consuming, labor-intensive, and error-prone; in fact, since most functional assays rely on relative measures, the definition of cutoffs between "mitochondrial" and "non-mitochondrial" PD subtypes is extremely challenging. In this context, the translation of a purely mitochondrial phenotyping approach into clinical trials for the stratification of large numbers of patients seems impractical.

Our study follows a different idea: the stratification of patients is entirely based on genetics and therefore defined by 'absolute' measures. This makes our approach robust, cost-effective and high-throughput compatible, as genetics can be easily assessed and provides 'definitive' data. Here, for the first time in the PD field, we functionally validated individual *OXPHOS*-PRS profiles in primary skin fibroblasts and the corresponding iPSC-derived neuronal progenitor cells established from genetically stratified iPD patients, showing significant differences in mitochondrial respiration between high- and low-risk groups (Fig 6). In primary skin fibroblasts, OCRs were significantly elevated in the high *OXPHOS*-PRS group—especially basal and ATP-linked respiration. It has been postulated that a similar phenotype, indicative of steady-state mitochondrial hyperactivity, may be an early event in PD pathogenesis, as suggested by increased neuronal viability and improved motor function in worms treated with
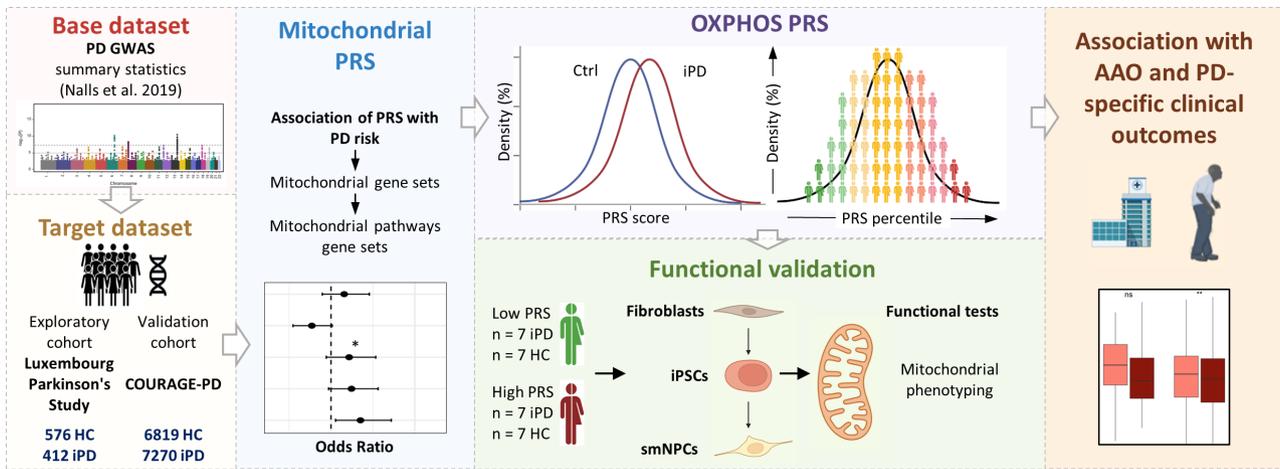
FIGURE 6: Study design and workflow. Created with BioRender.com.

the mitochondrial complex I inhibitor metformin.[56,57] Based on this model, hyperactive mitochondria may not only reduce the ability of the *OXPHOS* machinery to cope with a sudden increase in energy demand (e.g., in response to acute cellular stress), but also cause an excessive accumulation of ROS, which in turn increases oxidative damage and ultimately induces neurodegeneration. In this scenario, reduced ETC complex activity and impaired mitochondrial respiration—commonly observed in peripheral tissues and *post-mortem* brains of PD patients—would be late endpoint phenotypes, caused by ROS-mediated damage of mitochondrial complex I.[58] However, in the current study, increased mitochondrial respiration in fibroblasts with high *OXPHOS*-PRS was not accompanied by enhanced ROS production, likely due to the activation of compensatory mechanisms resulting in increased scavenging capacity.[59] High OCRs may also reflect the specific metabolism of the cells or tissues studied, including their ability to cope with mitochondrial dysfunction and to ensure ATP production. Similar to our findings, mitochondrial respiration was found to be significantly higher in Parkin-mutant fibroblasts compared to controls,[60,61] and mitochondrial hyperactivity was also observed in lymphoblasts from iPD patients.[62] In these studies, high OCRs were not accompanied by alterations in mitochondrial membrane potential or mtDNA copy number,[60,62] which is in line with our observations and further supports our stratification approach based on nuclear-encoded mitochondrial genes.

The results obtained in dermal fibroblasts are certainly informative and help to identify biological processes and molecular alterations also playing a relevant role in the neuronal environment, but their gene expression profile, metabolic adaptation to stress and signaling pathways strongly differ from that of neurons.[63] Moreover, the epigenetic changes that occur during somatic cell reprogramming to iPSCs and the subsequent differentiation into neuronal precursors could lead to opposing results between primary skin fibroblasts and smNPCs.[64] In accordance with this, mitochondrial respiration in iPSC-derived neuronal progenitor cells established from the corresponding reprogrammed fibroblasts was very similar between low and high *OXPHOS*-PRS groups. However, when forced to use OXPHOS instead of glycolysis to produce ATP (i.e., in galactose medium), smNPCs derived from iPD patients with high *OXPHOS*-PRSs displayed a significant reduction in their OCRs compared to the low *OXPHOS*-PRS group. Importantly, the degree of mitochondrial dysfunction in smNPCs from iPD patients with high *OXPHOS*-PRSs was comparable to that observed in cells from autosomal recessive PD patients carrying *PINK1* loss-of-function variants (see Fig 4). Of note, *PINK1*-PD is typically characterized by early onset and long disease duration, a phenotype that—according to our findings—is also observed in iPD patients with high *OXPHOS*-PRSs. Interestingly, smNPCs from sporadic PD patients with high *OXPHOS*-PRS displayed no significant differences in mitochondrial respiration compared to the control groups (either with low or high *OXPHOS*-PRS). This further highlights the capacity of our stratification approach based on *OXPHOS*-PRS to identify, among the heterogenous group of sporadic PD patients, those individuals with altered mitochondrial function who will benefit the most from therapies targeting mitochondria. Indeed, based on insights into the pathophysiology of neurodegeneration in PD, mitochondria early emerged as a potential therapeutic target for disease-modifying treatments (DMTs).[65] However, all clinical trials focusing on mitochondrially active compounds in PD (e.g., coenzyme Q10) were inconclusive, raising doubts about the validity of the concept of applying DMTs to unselected patient groups given the complex and heterogeneous nature of

PD.[66] Therefore, more recently, first clinical trials have been initiated, using genetic stratification strategies to define subgroups of PD patients, for example, carriers of rare variants in genes associated with mitochondrial dyshomeostasis and early-onset forms of monogenic PD.[67] If such approaches were successful, it would be still a very limited subgroup of PD patients that could benefit from these efforts. Thus, our robust and high-throughput compatible *OXPHOS*-PRS strategy may address the current needs for more focused DMT trials directed to sporadic iPD patients with an underlying, genetically defined, mitochondrial phenotype, who may benefit from drugs specifically targeting the respiratory chain activity. Such an approach, coupled with compounds that have shown ample preclinical and clinical evidence of targeting mitochondrial OXPHOS defects,[68] may be effective even if a given drug has previously failed in trials involving unselected PD patient groups. In accordance with this, retrospectively applying our *OXPHOS*-PRS approach to a double-blind, randomized trial in PD using UDCA, a naturally occurring bile acid shown to rescue mitochondrial function,[18] we found that UDCA-treated iPD patients with high *OXPHOS*-PRS had the greatest improvement in brain bioenergetics as quantified by 31P-MRS. In contrast, those patients in the placebo group who had the highest *OXPHOS*-PRS had the most marked worsening in their Gibbs free energy (reflecting ATP hydrolysis). Due to the limited number of study participants in some PRS groups and the retrospective exploratory nature of the analysis, we must acknowledge that these findings need to be confirmed in larger datasets, which would then also need to be adequately powered to allow correlation with a possible clinical effect. However, these results further corroborate the potential of our functionally validated genetic stratification approach and highlight the possibility to enrich future clinical trials of mitochondrially active drugs with iPD patients who have a high *OXPHOS*-PRS. Finally, as increased mitochondrial genetic risk is often associated with early-onset PD forms, individuals with very high *OXPHOS*-PRS could also represent a suitable target for preventative therapies.

Although the association between *OXPHOS*-PRS and PD risk is weaker than that observed with the whole-genome PD-PRS (see Fig 1), narrowing specific pathways—with fewer genes, but still significant effect—may shed new light on potential molecular mechanisms underlying PD pathogenesis. Thus, unlike the whole-genome PD-PRS, we believe that our genetic stratification approach based on *OXPHOS*-PRS represents a "precision tool" that may have a considerable impact on personalized medicine in PD. Another limitation of this study is the relatively small size of the Luxembourg Parkinson's Study cohort, which decreased the statistical power of our analyses; therefore, one could speculate that individuals with extreme *OXPHOS*-PRS values may not be in the top/bottom ranks of a larger cohort. This would explain why the inverse association between *OXPHOS*-PRS and AAO was only statistically significant in iPD patients from the large COURAGE-PD dataset, whereas the differences, although consistent (and corroborated by the correlation analysis), did not reach statistical relevance in the Luxembourg Parkinson's Study. It is worth mentioning that also whole-genome PRSs were previously found to be associated with earlier AAO,[69,70] whereas another study reported a positive correlation between mitochondrial PRSs and PD AAO.[14] While such conflicting results may simply be attributed to the different sizes of gene-sets used, it should be noted that monogenic PD forms with predominant mitochondrial pathogenesis (e.g., PINK1-PD) are also typically characterized by an early AAO. Importantly, our findings indicate that iPD patients with high *OXPHOS*-PRS are not only clinically, but also functionally similar to PINK1-PD patients. Functional validation of *OXPHOS*-PRSs in a larger number of iPD patients from additional large and deep-phenotyped PD cohorts are warranted to further explore the relationship between genetic stratification and the development of PD-associated clinical outcomes. On the other hand, available genetic information, clinical data and, at least in part, biospecimens from the subjects longitudinally followed in the Luxembourg Parkinson's Study, make this monocentric cohort quite unique, and the concomitant assessment of PD phenotypes, environmental risk factors and omics data could be integrated with *OXPHOS*-PRS to improve stratification accuracy of iPD patients. Combining genetic analyses, experimental validation studies and clinical assessment, all from the same individuals, certainly goes far beyond existing work, and provides a novel concept for precision medicine that is relevant for physicians and researchers engaged in translating fundamental research into therapeutic intervention for the treatment of neurodegenerative diseases.

Acknowledgements

Author Contributions

G.A., Z.L., D.G., N.D., C.K., E.G., T.F., O.B., M.S., R.K., P.M., and A.G. contributed to the conception and design of the study. G.A., Z.L., T.P., A.V., A.B., S.D., L.P., P.A., I.B., D.R.B., A.A.K.S., P.S., the NCER-PD consortium, and the COURAGE-PD consortium contributed to the acquisition and analysis of data. G.A., Z.L., T.P., L.P., R.K., P.M., and A.G. contributed to drafting the text or preparing the figures.

Potential Conflicts of Interest

The University of Luxembourg has filed the patent No. LU502780 "METHODS FOR STRATIFICATION OF PARKINSON'S DISEASE PATIENTS, SYSTEMS AND USES THEREOF". GA, ZL, RK, PM and AG are listed as inventors.

Data availability

Genetic and clinical data for this manuscript are not publicly available as they are linked to the internal regulations of the Luxembourg Parkinson's Study and COURAGE-PD. Requests for accessing the datasets can be directed to request.ncer-pd@uni.lu and courage@hih-mail.neurologie.uni-tuebingen.de, where dedicated data access committees review the requests and conclude data sharing agreements with prospective users.

Functional data are publicly available under the following link: https://zenodo.org/record/7973685.

References

1. Ascherio A, Schwarzschild MA. The epidemiology of Parkinson's disease: risk factors and prevention. Lancet Neurol 2016;15:1257–1272.
2. Jankovic J, Tan EK. Parkinson's disease: etiopathogenesis and treatment. J Neurol Neurosurg Psychiatry 2020;91:795–808.
3. Lesage S, Brice A. Parkinson's disease: from monogenic forms to genetic susceptibility factors. Hum Mol Genet 2009;18:R48–R59.
4. Nalls MA, Blauwendraat C, Vallerga CL, et al. Identification of novel risk loci, causal insights, and heritable risk for Parkinson's disease: a meta-analysis of genome-wide association studies. Lancet Neurol 2019;18:1091–1102.
5. Dehestani M, Liu H, Gasser T. Polygenic risk scores contribute to personalized medicine of Parkinson's disease. J Pers Med 2021;11:1030.
6. Choi SW, Mak TS-H, O'Reilly PF. Tutorial: a guide to performing polygenic risk score analyses. Nat Protoc 2020;15:2759–2772.
7. Sherer TB, Richardson JR, Testa CM, et al. Mechanism of toxicity of pesticides acting at complex I: relevance to environmental etiologies of Parkinson's disease. J Neurochem 2007;100:1469–1479.
8. González-Rodríguez P, Zampese E, Stout KA, et al. Disruption of mitochondrial complex I induces progressive parkinsonism. Nature 2021;599:650–656.
9. Malpartida AB, Williamson M, Narendra DP, et al. Mitochondrial dysfunction and mitophagy in Parkinson's disease: from mechanism to therapy. Trends Biochem Sci 2021;46:329–343.
10. Schapira AHV, Cooper JM, Dexter D, et al. Mitochondrial complex I deficiency in Parkinson's disease. Lancet 1989;333:1269.
11. Angelova PR, Abramov AY. Role of mitochondrial ROS in the brain: from physiology to neurodegeneration. FEBS Lett 2018;592:692–702.
12. Bender A, Krishnan KJ, Morris CM, et al. High levels of mitochondrial DNA deletions in substantia nigra neurons in aging and Parkinson disease. Nat Genet 2006;38:515–517.
13. Burbulla LF, Krüger R. Converging environmental and genetic pathways in the pathogenesis of Parkinson's disease. J Neurol Sci 2011;306:1–8.
14. Billingsley KJ, Barbosa IA, Bandrés-Ciga S, et al. Mitochondria function associated genes contribute to Parkinson's disease risk and later age at onset. npj Parkinsons Dis. 2019;5:8.
15. Hipp G, Vaillant M, Diederich NJ, et al. The Luxembourg Parkinson's study: a comprehensive approach for stratification and early diagnosis. Front Aging Neurosci 2018;10:326.
16. Domenighetti C, Sugier P, Ashok Kumar Sreelatha A, et al. Dairy intake and Parkinson's disease: a mendelian randomization study. Mov Disord 2022;37:857–864.
17. Grover S, Kumar-Sreelatha AA, Bobbili DR, et al. Replication of a novel Parkinson's locus in a European ancestry population. Mov Disord 2021;36:1689–1695.
18. Payne T, Appleby M, Buckley E, et al. A double-blind, randomized, placebo-controlled trial of Ursodeoxycholic acid (UDCA) in Parkinson's disease. Mov Disord 2023;38:1493–1502.
19. Payne T, Burgess T, Bradley S, et al. Multimodal assessment of mitochondrial function in Parkinson's disease. Brain 2024;147:267–280.
20. Litvan I, Bhatia KP, Burn DJ, et al. SIC task force appraisal of clinical diagnostic criteria for parkinsonian disorders. Mov Disord 2003;18:467–486.
21. Blauwendraat C, Faghri F, Pihlstrom L, et al. NeuroChip, an updated version of the NeuroX genotyping platform to rapidly screen for variants associated with neurological diseases. Neurobiol Aging 2017;57:247.e9–247.e13.

22. Chang CC, Chow CC, Tellier LC, et al. Second-generation PLINK: rising to the challenge of larger and richer datasets. GigaScience 2015; 4:7.

23. Landoulsi Z, Pachchek S, Bobbili DR, et al. Genetic landscape of Parkinson's disease and related diseases in Luxembourg. Front Aging Neurosci 2023;15:1282174.

24. Pachchek S, Landoulsi Z, Pavelka L, et al. Author correction: accurate long-read sequencing identified GBA1 as major risk factor in the Luxembourgish Parkinson's study. npj Parkinsons Dis 2023;9:168.

25. Das S, Forer L, Schönherr S, et al. Next-generation genotype imputation service and methods. Nat Genet 2016;48:1284–1287.

26. Rath S, Sharma R, Gupta R, et al. MitoCarta3.0: an updated mitochondrial proteome now with sub-organelle localization and pathway annotations. Nucleic Acids Res 2021;49:D1541–D1547.

27. Choi SW, O'Reilly PF. PRSice-2: polygenic risk score software for biobank-scale data. GigaScience 2019;8:giz082.

28. Cai L, Wheeler E, Kerrison ND, et al. Genome-wide association analysis of type 2 diabetes in the EPIC-InterAct study. Sci Data 2020; 7:393.

29. Bigdeli TB, Fanous AH, Li Y, et al. Genome-wide association studies of schizophrenia and bipolar disorder in a diverse cohort of US veterans. Schizophr Bull 2021;47:517–529.

30. Kunkle BW, Grenier-Boley B, Sims R, et al. Genetic meta-analysis of diagnosed Alzheimer's disease identifies new risk loci and implicates Aβ, tau, immunity and lipid processing. Nat Genet 2019;51:414–430.

31. Reinhardt P, Glatza M, Hemmer K, et al. Derivation and expansion using only small molecules of human neural progenitors for neurodegenerative disease modeling. PLoS One 2013;8:e59252.

32. Jarazo J, Barmpa K, Modamio J, et al. Parkinson's disease phenotypes in patient neuronal cultures and brain organoids improved by 2-HYDROXYPROPYL-β-CYCLODEXTRIN treatment. Mov Disord 2022;37: 80–94.

33. Gu X, Ma Y, Liu Y, Wan Q. Measurement of mitochondrial respiration in adherent cells by seahorse XF96 cell Mito stress test. STAR Protoc 2021;2:100245.

34. Swerdlow RH, Lezi E, Aires D, Lu J. Glycolysis–respiration relationships in a neuroblastoma cell line. Biochim Biophys Acta, Gen Subj 2013;1830:2891–2898.

35. Maston GA, Evans SK, Green MR. Transcriptional regulatory elements in the human genome. Annu Rev Genom Hum Genet 2006;7: 29–59.

36. Bandres-Ciga S, Saez-Atienzar S, Kim JJ, et al. Large-scale pathway specific polygenic risk and transcriptomic community network analysis identifies novel functional pathways in Parkinson disease. Acta Neuropathol 2020;140:341–358.

37. Jung S-H, Kim H-R, Chun MY, et al. Transferability of Alzheimer disease polygenic risk score across populations and its association with Alzheimer disease-related phenotypes. JAMA Netw Open 2022;5: e2247162.

38. Kachuri L, Graff RE, Smith-Byrne K, et al. Pan-cancer analysis demonstrates that integrating polygenic risk scores with modifiable risk factors improves risk prediction. Nat Commun 2020;11:6084.

39. Mitchell P. Coupling of phosphorylation to electron and hydrogen transfer by a Chemi-osmotic type of mechanism. Nature 1961;191: 144–148.

40. Chen H, Chomyn A, Chan DC. Disruption of fusion results in mitochondrial heterogeneity and dysfunction. J Biol Chem 2005;280: 26185–26192.

41. Yao C-H, Wang R, Wang Y, et al. Mitochondrial fusion supports increased oxidative phosphorylation during cell proliferation. eLife 2019;8:e41351.

42. Grünewald A, Rygiel KA, Hepplewhite PD, et al. Mitochondrial DNA depletion in respiratory chain–deficient Parkinson disease neurons. Ann Neurol 2016;79:366–378.

43. Tang JX, Thompson K, Taylor RW, Oláhová M. Mitochondrial OXPHOS biogenesis: Co-regulation of protein synthesis, import, and assembly pathways. Int J Mol Sci 2020;21:3820.

44. Borsche M, König IR, Delcambre S, et al. Mitochondrial damage-associated inflammation highlights biomarkers in PRKN/PINK1 parkinsonism. Brain 2020;143:3041–3051.

45. Sliter DA, Martinez J, Hao L, et al. Parkin and PINK1 mitigate STING-induced inflammation. Nature 2018;561:258–262.

46. Candelario KM, Shuttleworth CW, Cunningham LA. Neural stem/progenitor cells display a low requirement for oxidative metabolism independent of hypoxia inducible factor-1alpha expression. J Neurochem 2013;125:420–429.

47. Blauwendraat C, Nalls MA, Singleton AB. The genetic architecture of Parkinson's disease. Lancet Neurol 2020;19:170–178.

48. Ohnmacht J, May P, Sinkkonen L, Krüger R. Missing heritability in Parkinson's disease: the emerging role of non-coding genetic variation. J Neural Transm 2020;127:729–748.

49. Paliwal D, McInerney TW, Pa J, et al. Mitochondrial pathway polygenic risk scores are associated with Alzheimer's disease. Neurobiol Aging 2021;108:213–222.

50. Khera AV, Chaffin M, Aragam KG, et al. Genome-wide polygenic scores for common diseases identify individuals with risk equivalent to monogenic mutations. Nat Genet 2018;50:1219–1224.

51. Landi I, Kaji DA, Cotter L, et al. Prognostic value of polygenic risk scores for adults with psychosis. Nat Med 2021;27:1576–1581.

52. Leonenko G, Baker E, Stevenson-Hoare J, et al. Identifying individuals with high risk of Alzheimer's disease using polygenic risk scores. Nat Commun 2021;12:4506.

53. Dehestani M, Liu H, Sreelatha AAK, et al. Mitochondrial and autophagy-lysosomal pathway polygenic risk scores predict Parkinson's disease. Mol Cell Neurosci 2022;121:103751.

54. Adeyemo A, Balaconis MK, Darnes DR, et al. Responsible use of polygenic risk scores in the clinic: potential benefits, risks and gaps. Nat Med 2021;27:1876–1884.

55. Carling PJ, Mortiboys H, Green C, et al. Deep phenotyping of peripheral tissue facilitates mechanistic disease stratification in sporadic Parkinson's disease. Prog Neurobiol 2020;187:101772.

56. Mor DE, Sohrabi S, Kaletsky R, et al. Metformin rescues Parkinson's disease phenotypes caused by hyperactive mitochondria. Proc Natl Acad Sci U S A 2020;117:26438–26447.

57. Mor DE, Murphy CT. Mitochondrial hyperactivity as a potential therapeutic target in Parkinson's disease. Transl Med Aging 2020;4: 117–120.

58. Keeney PM. Parkinson's disease brain mitochondrial complex I has oxidatively damaged subunits and is functionally impaired and misassembled. J Neurosci 2006;26:5256–5264.

59. Dias V, Junn E, Mouradian MM. The role of oxidative stress in Parkinson's disease. J Parkinsons Dis 2013;3:461–491.

60. Haylett W, Swart C, van der Westhuizen F, et al. Altered mitochondrial respiration and other features of mitochondrial function in *parkin*-mutant fibroblasts from Parkinson's disease patients. Parkinson's Dis 2016;2016:1–11.

61. Zanellati MC, Monti V, Barzaghi C, et al. Mitochondrial dysfunction in Parkinson disease: evidence in mutant PARK2 fibroblasts. Front Genet 2015;6:128375.

62. Annesley SJ, Lay ST, De Piazza SW, et al. Immortalized Parkinson's disease lymphocytes have enhanced mitochondrial respiratory activity. Dis Model Mech 2016;9:1295–1305.

63. Auburger G, Klinkenberg M, Drost J, et al. Primary skin fibroblasts as a model of Parkinson's disease. Mol Neurobiol 2012;46:20–27.

64. Kim D-Y, Rhee I, Paik J. Metabolic circuits in neural stem cells. Cell Mol Life Sci 2014;71:4221–4241.

65. Chaturvedi RK, Beal MF. Mitochondrial approaches for neuroprotection. Ann N Y Acad Sci 2008;1147:395–412.

66. The Parkinson Study Group QE3 Investigators, Beal MF, Oakes D, et al. A randomized clinical trial of high-dosage coenzyme Q10 in early Parkinson disease: No evidence of benefit. JAMA Neurol 2014; 71:543–552.

67. Prasuhn J, Kasten M, Vos M, et al. The use of vitamin K2 in patients with Parkinson's disease and mitochondrial dysfunction (PD-K2): a Theranostic pilot study in a placebo-controlled parallel group design. Front Neurol 2021;11:592104.

68. Kalyanaraman B. Teaching the basics of repurposing mitochondria-targeted drugs: from Parkinson's disease to cancer and back to Parkinson's disease. Redox Biol 2020;36:101665.

69. Blauwendraat C, Heilbron K, Vallerga CL, et al. Parkinson's disease age at onset genome-wide association study: defining heritability, genetic loci, and α-synuclein mechanisms. Mov Disord 2019;34: 866–875.

70. Huang Y, Chen Q, Wang Z, et al. Risk factors associated with age at onset of Parkinson's disease in the UK biobank. npj Parkinson's Dis 2024;10:3.

71. Antony PMA, Kondratyeva O, Mommaerts K, et al. Fibroblast mitochondria in idiopathic Parkinson's disease display morphological changes and enhanced resistance to depolarization. Sci Rep 2020; 10:1569.